

4-2018

3D Modeling and Animation of the Temporomandibular Joint (TMJ) of a Human Male with Implications for the Study of TMJ Dysfunction

Breigh Sonnier

Follow this and additional works at: https://repository.lsu.edu/honors_etd



Part of the [Biology Commons](#)

Recommended Citation

Sonnier, Breigh, "3D Modeling and Animation of the Temporomandibular Joint (TMJ) of a Human Male with Implications for the Study of TMJ Dysfunction" (2018). *Honors Theses*. 1448.
https://repository.lsu.edu/honors_etd/1448

This Thesis is brought to you for free and open access by the Ogden Honors College at LSU Scholarly Repository. It has been accepted for inclusion in Honors Theses by an authorized administrator of LSU Scholarly Repository. For more information, please contact ir@lsu.edu.

3D Modeling and Animation of the Temporomandibular Joint (TMJ) of a Human Male with Implications
for the Study of TMJ Dysfunction

by

Breigh Sonnier

Undergraduate honors thesis under the direction of

Dr. Dominique G. Homberger

Department of Biological Sciences

Submitted to the LSU Roger Hadfield Ogden Honors College in partial fulfillment of
the Upper Division Honors Program.

April 2018

Louisiana State University
& Agricultural and Mechanical College
Baton Rouge, Louisiana

Contents

Abstract.....	3
Introduction	4
Background	5
The Temporomandibular Joint.....	5
Sutures	8
Hyoid	8
Muscles	9
Temporomandibular Joint Dysfunction	11
Materials and Methods.....	12
Segmentation.....	12
Animation.....	15
Creation of a Surface View.....	15
Replacement of old animation.....	15
Character Rigging	16
Results.....	16
The Temporomandibular Joint.....	16
Sagittal Suture	16
Discussion.....	17
The Temporomandibular Joint.....	17
Sagittal Suture	18
General Discussion	19
References	20
Figure Legend.....	24
Figures.....	26

Abstract

Temporomandibular joint dysfunction (TMD) affects approximately 60-70% of the U.S. population, but the precise mechanisms underlying the causes of TMD are not well understood. We hypothesize that there is a biomechanical cause for TMD and have developed a 3D model that can be manipulated to simulate different positions and postures that may adversely affect the temporomandibular joint (TMJ). To create such a 3D model, donated x-ray CT data of the head, neck, and shoulders of a middle aged were analyzed using the visualization software program Avizo 9.2.0[®]. The skull, mandible, teeth, and hyoid bone were manually segmented (i.e., marked as individual elements). The segmented 3D data were exported to the animation software Maya 2017[®] and graphically linked through a process known as character rigging so that the individual skeletal elements could be moved into various positions. This animated 3D model allows the study of various positions and body postures and their effects on the TMJ without having to resort to clinical observations with their ethically dictated limitations.

Introduction

The temporomandibular joint (TMJ) is formed by the temporal bone and mandibular condyle and allows the jaw movements necessary for chewing, speaking, yawning and other activities involving the mouth. Dysfunction of the TMJ is very common, with approximately 65% of the U.S. population reporting symptoms of the disorder (Dutton 2012). Despite this, little is known about the causes for temporomandibular joint dysfunction (TMD). We hypothesize that there is a biomechanical cause for TMD and that by understanding the biomechanics of the jaw, better treatments for the condition can be developed.

The aim of this study was to create an animated 3D model of the human jaw apparatus, which will eventually be used to examine and compare the forces involved in the movements of healthy and dysfunctional TMJs. Previous work on the shoulder suspension apparatus (Osborn 2013; Osborn & Homberger 2015; Osborn *et al.* in prep.) has shown that it is feasible to compute the forces exerted on a skeleto-muscular system through the method of 3D free-body force analyses. By applying this method to the animated 3D model in various jaw positions, the changes in the force regime throughout the process of opening and closing the jaw can be analyzed. Modeling the forces acting on the TMJ is a necessary step towards a better understanding of the biomechanics of the joint as a basis for clinical investigations.

Background

The Temporomandibular Joint

The temporomandibular joint is formed by the articulation of two of the temporal bone and mandible. The temporal bone is located on the lateral aspect of the skull, inferior to the parietal bone, and extends posteriorly from the greater wing of the sphenoid bone to the lambdoidal suture. The sphenoid bone is part of the basicranium and has a pair of lateral projections, called the greater wings, which cover the sides of the braincase just behind the orbits. The spine located on the greater wings serves as the attachment point for the lateral pterygoid muscle (Gray 1918). The temporal bone is comprised of five major components: The squamosal bone (Squama), the petrosal bone, the mastoid process, the tympanic portion, the styloid process, and the zygomatic process (Fig. 1; Williams 1995; Homberger & Walker 2004). The squamosal is the thin superior portion of the temporal bone and bears the temporal fossa, which serves as the attachment site for the temporalis muscle. The petrosal bone is the portion of the temporal bone that extends into the skull and houses the inner ear. It is the densest bone of the human body. The mastoid process is a thick postero-lateral bony projection of the petrosal bone, which serves as the attachment site for the sternocleidomastoid muscle (Homberger & Walker 2004; Osborn 2013; Osborn & Homberger 2015). The tympanic portion is the area just posterior to the TMJ and surrounds the external acoustic meatus. The styloid process is an inferior projection of the temporal bone to which the stylohyoid ligament attaches. It is a remnant of a part of the ossicular chain that suspends the hyoid to the skull in other mammals. In humans, the bilateral stylohyoid ligaments suspend the hyoid bone from the skull (Homberger & Walker 2004). The zygomatic process is an anterior projection of the

squamous portion of the temporal bone, which articulates anteriorly with the zygomatic bone (Gray 1918). Together, the zygomatic bone and zygomatic process of the temporal bone form the zygomatic arch. At the posterior end of the zygomatic process lies the mandibular fossa, which is bounded anteriorly by the articular tubercle. The sinusoidal surface formed by the articular tubercle and mandibular fossa is the surface along which the mandibular condyle and articular disc travel during jaw movements (Fig. 2; Williams 1995). When the jaw opens, the mandibular condyle first undergoes an anterior angular rotation within the mandibular fossa and then translates anteriorly together with the articular disc over the articular tubercle (Gray 1918).

While the main skeletal elements of the human jaw apparatus are the skull, mandible, and teeth, the hyoid and sagittal suture were also modeled as they are related peripherally to the function of the TMJ.

The mandible is composed of the body and the ramus (Fig. 3). The body of the mandible is the horizontal, parabolic portion bearing the teeth, whereas the ramus is the thick, vertical region. The angle formed between the body and ramus is called the gonial angle. Two processes extend superiorly from the ramus: The coronoid and the condyloid process. The more anterior one is the coronoid process, which serves as the attachment site for the temporalis and masseter muscles. The more posterior condyloid process (mandibular condyle) is the attachment site for the lateral pterygoid muscle and bears the articular facet for the TMJ (Williams 1995).

Within the TMJ, between the mandibular fossa and mandibular condyle, lies a biconcave fibrocartilaginous articular disc, which acts as the gliding surface for the joint (Williams 1995).

The center of the disc is devoid of blood vessels and nerves, while the periphery of the disc is richly vascularized and innervated (Patel & Collins 2016). This is consistent with the notion that the center of the disc is the load-bearing portion (Patel & Collins 2016). The disc is held in place by capsular fibers that attach it loosely to the fibrous joint capsule that surrounds the entire joint, as well as by several ligaments.

The articular disc separates the joint into superior and inferior compartments (Gray 1918). Each compartment is lined with its own synovial membrane (Fig. 2), which secretes the synovial fluid, provides nutrients to the articular cartilage, and lubricates the joint (Hombberger & Walker 2004). The synovial membranes of each compartment attach to the edges of the disc. The articular cartilage of the TMJ differs from the articular cartilage of other joints of the human body, which is hyaline cartilage, a glassy, white cartilage with a matrix composition of type II collagen fibers and the proteoglycan aggrecan (Freemont & Hoyland 2006). The articular surfaces of the TMJ, in contrast, consist of fibrocartilage (Williams 1995; Patel & Collins 2016), which contains both type I and type II collagen and aggrecan (Freemont & Hoyland 2006). Fibrocartilage is tougher and more flexible than hyaline cartilage and, because it is vascularized, is able to be repaired and remodeled in contrast to hyaline cartilage (Freemont & Hoyland 2006; Patel & Collins 2016).

The joint is stabilized through several ligaments (Fig. 4). The temporomandibular ligament attaches to the posterior region of the zygomatic process and to the lateral aspect of the mandibular condyle. The stylomandibular ligament attaches to the styloid process of the skull and the gonial angle of the mandible. The sphenomandibular ligament attaches to the spine on the greater wings of the sphenoid and to the lateral aspect of the mandible, superior

to the mandibular foramen. There are also two collateral ligaments that attach the disc to the mandibular condyle medially and laterally. Also associated with the TMJ are the otomandibular ligaments, which include the anterior malleolar ligament and the discomalleolar ligament. The latter passes through the petrotympanic fissure and connects the malleus of the middle ear to the posterior part of the articular disc and joint capsule. The anterior malleolar ligament connects the malleus to the sphenomandibular ligament. The otomandibular ligaments are responsible for the TMD-related symptoms of the middle ear (e.g., dizziness, tinnitus, hyperacusis) (Aristeguieta *et al.* 2009).

Sutures

The flat bones of the skull are connected to one another through fibrous joints called sutures. There are four major sutures of the adult human cranium: The coronal suture separating the frontal bone from the paired parietal bones; the sagittal suture separating the two parietal bones; the squamosal sutures separating the temporal bones from the parietal bones; and the lambdoidal suture separating the occipital bone from the temporal and parietal bones. Sutures allow a small amount of movement between the skull bones and, thereby, confer a certain elasticity to the skull and provide a mechanism for the absorption of compressive and tensile forces generated during mastication (Herring 2008).

Hyoid

The hyoid bone in humans is composed of three parts: The body, the greater cornua, and the lesser cornua (Fig. 5). The body of the hyoid is the flat, rectangular, central segment of the bone. The greater cornua project postero-superiorly from either side of the body of the

hyoid. The lesser cornua are reduced to small projections extending superiorly from the base of the greater cornua. The hyoid does not articulate with other bones. Instead, the lesser cornua are suspended *via* the stylohyoid ligaments to the styloid processes of the temporal bones (Gray 1918). The lateral thyrohyoid ligaments attach to the posterior ends of the greater cornua and to the thyroid cartilage of the larynx, and the medial thyrohyoid ligament attaches inferiorly to the body of the hyoid and to the thyroid cartilage. The hyoid acts as an attachment site for the muscles responsible for the movements of the tongue (Williams 1995). It is involved in vocalization and swallowing (Lieberman *et al.* 2001) and in jaw movements through the digastric muscle, which is responsible for the depression of the mandible

Muscles

There are five major muscles involved in mastication. These include the temporalis, the masseter, the medial pterygoid, the lateral pterygoid, and the digastric muscles. The temporalis muscle is a large, fan-shaped muscle that originates from the temporal fossa and passes internally to the zygomatic arch to insert on the coronoid process and the anterior side of the mandibular ramus (Fig. 6). It is divided into two parts based on the direction of their muscle fibers. The anterior portion with nearly vertical fibers elevates the mandible when the mouth is being closed and aids in protruding the mandible. The fibers of the posterior portion are oriented more horizontally and retract the mandible (Williams 1995).

The masseter muscle has a superficial and a deep head. The superficial head is larger and originates from the anterior portion of the zygomatic arch. It inserts on the gonial angle and lower portion of the ramus (Fig. 7). The deep head originates from the posterior portion of the zygomatic arch and inserts on the upper half of the ramus and coronoid process (Fig. 7). The

masseter muscle elevates the mandible and can aid in lateral excursions by contracting unilaterally (Williams 1995).

The medial pterygoid muscle is located on the medial surface of the ramus. It originates on the pterygoid plate and palate and inserts on the ramus and gonial angle of the mandible where it joins with the insertion of the masseter muscle (Fig. 8), making the combined muscle mass a powerful elevator of the jaw. The medial pterygoid muscle also plays a role in protrusion of the jaw and can aid in lateral excursions by contracting only one side of the muscle (Williams 1995).

The lateral pterygoid muscle is divided into a superior and an inferior head. The latter originates on the sphenoid bone and inserts on the condyloid process. The superior head originates on the pterygoid plate and inserts mostly on the anterior portion of the articular capsule (Fig. 8). A few fibers have been found to insert on the articular disc itself in some individuals (Patel & Collins 2016).

The digastric muscle has two bellies that are connected in the middle by the round intermediate tendon (Fig. 9). It has two origins on the mandibular symphysis and the mastoid process. A fibrous loop passing over the intermediate tendon allows the muscle to insert on the greater cornu of the hyoid. The digastric muscle is part of a group of muscles referred to as the suprahyoid muscles which function to elevate the hyoid during speech and swallowing. The digastric muscle also depresses the mandible to open the jaw and aids in the retraction of the jaw (Williams 1995).

Temporomandibular Joint Dysfunction

Approximately 65% of the population presents with at least one sign of temporomandibular joint dysfunction (TMD). Of these 65%, 25% are aware of it and report the symptoms, but only 5% will seek treatment for the condition (Dutton 2012). TMD refers to a wide range of disorders of the TMJ. These disorders can be classified into two major types, arthrogenous and myogenous (Rios & Berman 2017). In arthrogenous TMD, the dysfunction is caused by articular disease, such as disc derangement, chronic recurrent dislocations, degenerative joint disorders, systemic arthritis, ankylosis, infections, and neoplasia. In myogenous TMD, the dysfunction is a result of myofascial pain and dysfunction of the masticatory muscles caused by bruxism, daytime clenching, muscle hyperactivity, or malocclusion. There is often also a psychological component to myogenous TMD, and it is recommended to treat the condition using a biopsychosocial model that encompasses the treatment of not only the physical aspects of the disorder (e.g., bruxism, arthritis, craniofacial pain, etc.), but also the psychological factors, such as stress and anxiety, that contribute to the disorder (Rios & Berman 2017).

The most common cause of TMD is disc derangement. There are several stages of derangement as described by Rocabado (1991). The first stage occurs when the posterior ligament holding the disc in place is stretched beyond its normal range, allowing the disc to be positioned more anteriorly than normal. It is likely that Rocabado is referring to the posterior part of the fibers surrounding the disc that attach it to the temporal bone and mandible. The next stage occurs when the lateral collateral ligament is stretched, allowing the disc to slip medially. The derangement of the disc pushes the mandibular condyle to a more supero-

posterior position within the joint capsule. When the jaw opens, the mandibular condyle will often slip off the disc and then back onto it when the jaw is closed. This is what causes the clicking sound that is often associated with TMD. As the disorder progresses, it is possible for the disc to become trapped behind the mandibular condyle. At this stage, the mandibular condyle no longer glides over the surface of the disc at all and, therefore, no clicking sound is made. However, the jaw will often be restricted to opening only as far as the angular rotation of the condyle will allow, and damage to the cartilage may occur over time.

Materials and Methods

An animated 3D model of the skull, mandible and teeth of a human male was created based on donated x-ray CT data of the upper body of an adult, middle-aged male, who is a former athlete and had surgery to remove a tumor from the upper left side of his brain.

Segmentation

The 3D data were imported into the visualization software Avizo 9.2.0[®] to visualize and segment (i.e., mark as individual elements) the skull, mandible, teeth, and hyoid bone. The segmentation was done manually because the tools in Avizo[®]'s automated segmentation suite are not reliable for use with biological tissues. The density of bone is not uniform, which makes it impossible to use automation segmentation tools that rely on a consistent density of the material. Instead, a different threshold must be chosen for each structure that is being segmented. Thresholding refers to the process of choosing the range of materials that can be seen according to their densities. Further, the resolution of the CT scan affects the level of morphological detail that can be displayed. With a low-resolution scan, more data is contained

within each voxel because the voxels are larger, making smaller structures difficult to see. This is similar to what is seen in low resolution 2D pictures (Fig. 10).

The CT scan used was a medical grade scan and was relatively low in resolution. This makes it difficult to decide how to categorize voxels that are part of structures in close proximity to another structure or air (e.g., on the surface of a skull bone). The low resolution also makes it difficult to see structures that are smaller than the size of the voxels, such as the sutures on the skull and the gaps between the teeth. For these areas, it was necessary to evaluate each voxel individually in three orthographic planes (XY, XZ, YZ) using knowledge of the anatomy to contextualize it. This same technique has been used by paleoanthropologists when analyzing the data of fossil skulls filled with a mineral matrix that is similar in density to fossilized bone (Gunz 2014). The human eye is better able to contextualize the data and see beyond the given densities and determine to which structure the voxels belong.

The available CT data had been previously segmented and animated by undergraduate students in the course HNRS 3035 (3D Imaging) taught by Dr. Homberger at Louisiana State University. Because the skull, mandible, cervical vertebra, and upper limbs had been segmented using an automatic segmentation tool, the segmentations were messy and inaccurate, with materials from one bone frequently appearing in the bones adjacent to it. To correct this, the model was resegmented working sequentially through individual slices, and adjusting the threshold as needed to highlight the appropriate materials.

The lower threshold used for the superficial surface (compacta) of the braincase was set at 550 Hounsfield units (HU). For the border between the compacta and diploe, voxels over 700

HU were assigned to the compacta and voxels in the 650-700 HU range were evaluated individually.

The density of the area surrounding the sutures exhibited too much variability to use a single, consistent threshold during segmentation, and instead had to be individually evaluated. This was most likely a consequence of the shape and smaller size of the sutures compared to the size of the voxels of the CT scan.

The density of the mandible and hyoid bones were much more consistent. For the mandible, a threshold of 500 HU was chosen as the baseline, with voxels near this value being individually examined. A similar process was completed for the hyoid bone with the baseline threshold set at 350 HU. The thresholds were chosen by comparing the structures visible in the CT scan to the expected morphology.

The teeth were segmented as individual structures. The 2D orthoslices in the segmentation window were set to show materials in the range of 300-1700 HU, a range at which the teeth were clearly visible against the alveolar bone. A baseline threshold of 450 HU was used for the segmentation of the teeth. However, because the teeth sit within the alveolar bone, this threshold could not be used reliably for an automatic segmentation, and the borders of the teeth had to be evaluated individually. Near the crowns of the teeth, the resolution of the scan and radiographic noise from metal fillings in the individual's molars made the teeth appear fused together. In order to segment the teeth as individual units, a gap was artificially inserted using the expected anatomy of the teeth. The crowns of the molars were left unsegmented due to the radiographic noise created by the metal fillings, but could potentially be reconstructed using the expected anatomy.

Animation

The segmented materials were used to create a surface view in Avizo® that was exported to Maya® 2017 and animated according to the current understanding of the literature on the movements of the jaw (Gray 1918; Rocabado & Iglarsh 1991; Almodafr 2014).

Creation of a Surface View

On Avizo®'s project view, the label file containing the segmented data was selected and the "Generate Surface" tool was selected. All settings were left in their default positions, and "no smoothing" was selected before applying the tool. The new surface file was then selected and the "Create Surface View" tool was applied to visualize the surface. The surface file was again selected and the "Smooth Surface" tool was used. The number of iterations was changed to 10, and the tool was applied. The smoothed surface was then divided into the skull (with sutures and upper teeth included) and the mandible (with teeth included) using the buffer settings. The separated materials were exported and saved as Waveform (.obj) files.

Replacement of old animation

The file containing the previously completed animation was opened, and the new segmentation files, referred to in Maya as "meshes" were imported to replace the old meshes. To maintain the character rigging that had been built previously, the new meshes needed to be matched in size, shape, and position to the old meshes (Fig. 11A). To do this, both meshes were selected (new mesh, then old mesh) and the "Match Transformations" tool was applied (Modify → Match Transformations → Match All Transformations) (Fig. 11B; 11C). The old mesh was then replaced with the new mesh by selecting first the old mesh, and then the new mesh, and

using the “Replace Materials” tool (Modify → Replace Materials) (Fig. 11D; 11E). This process was repeated for both the skull and the mandible.

Character Rigging

To animate the skull, a single joint was created over the TMJ and constrained to the mandible so that the mandible would move when the joint handle was moved. A control was then created using a NURBS circle and constrained to the joint handle so that the control could be used to move the joint and, thereby, the mandible. Using the control, the mandibular condyle was set to pivot anteriorly 10° within the mandibular fossa, and then translate forward along the articular tubercle. These constraints were based on current literature describing the movement of the TMJ joint (Gray 1918; Rocabado & Iglarsh 1991; Almodafr 2014).

Results

The Temporomandibular Joint

The model created allowed the mandible to be mobilized into the various positions seen during the normal opening of the jaw. These positions include the resting position of mandibular condyle within the mandibular fossa (Fig. 12A; 12D), the position of the condyle after its angular rotation within the mandibular fossa (Fig. 12B; 12E), and the position of the condyle after its anterior translation over the articular tubercle (Fig. 12C; 12F).

Sagittal Suture

The individual whose x-ray CT data were used had previously had brain surgery to remove a tumor from the upper left side of the brain. During the surgery, a craniotomy was performed on the left parietal bone to grant the surgeons access to the brain and tumor. The

skull flap was replaced after the surgery using surgical clips, but never healed or ossified, leaving a large gap between the skull flap and the surrounding skull bones. The sagittal suture ossified along to the sagittal gap between the sagittal suture and the skull flap (Fig. 13 A-D).

Discussion

The Temporomandibular Joint

The created animated 3D model can be manipulated into the various configurations observed during normal and abnormal movements of the jaw. Modeled here is an estimation of the movements seen during the normal opening and closing of the jaw based on knowledge of the current literature regarding the movements of the jaw (Gray 1918; Rocabado and Iglarsh 1991; Almodafr 2014) (Fig. 12A-F). In order to model the actual movements made by the individual whose x-ray CT data were used, the images would need to be matched to individual frames of fluoroscopic videos of the same individual moving his jaw (for technical details, see Homberger 2017). Future studies using this technique would be able to model more movements, such as lateral excursions, protrusion, and retrusion, as well as the masticatory cycle.

The technique used to animate this model by basing the positions on knowledge of current literature can also be used to simulate abnormal configurations of the jaw. For example, studies by Rocabado (1991) and Ohmure *et al.* (2008) have shown that in a forward head posture, the mandibular condyle is positioned more posteriorly at rest than it is in normal posture. The model can also be used to demonstrate abnormal movements commonly seen in

patients with TMD, such as lateral excursions when opening the mouth (Rocabado & Iglarsh 1991).

The created 3D model contains only the bony elements of the TMJ. The articular disc, however, is an essential component of the functional TMJ and has been the focus of most temporomandibular joint dysfunction (TMD). The articular disc could not be included on this model because cartilage is not visible in x-ray CT data. However, an MRI of the TMJ would allow for its visualization. Using the method developed by Wood *et al.* (in press), the disc could be segmented and included in the animated 3D model. This would allow the normal movements of the disc to be modeled, as well as the various derangements of the disc seen in patients with TMD.

The model can also be used to compute the forces exerted on the joint in normal and pathological positions. Previous work (Osborn 2013; Osborn & Homberger 2015; Osborn *et al.* in prep.) has been done on the shoulder suspension apparatus in humans using 3D free-body force analyses to compute the forces exerted by the fasciae and muscles to maintain equilibrium at rest. This technique can be applied to the TMJ to analyze how the force regime on the joint changes with different postures, such as forward head posture.

Sagittal Suture

When the jaw creates a unilateral bite force, as in chewing, the contraction of the temporalis muscle subjects the TMJ and the skull on the ipsilateral side to compressive forces, and the TMJ and the skull with its sutures on the contralateral side to tensile forces (Herring 2008; Herring *et al.* 2001). The tensile forces are relieved by the sutures of the skull, which

allow the skull bones to move slightly. When the individual, whose CT data were used, had brain surgery, a portion of his skull was removed and then later secured back into place with surgical clips. A large gap was created around the surgical site that presumably allowed for more movement than the sagittal suture, and thereby became the functional “suture” of the skull. This allowed the sagittal suture to be immobile for long enough so that it ossified along the length of the skull flap (Fig 13A-D).

General Discussion

As imaging techniques improve, the fields of science and medicine will become more suited to the study of the individual differences seen among humans, rather than models based on generalizations and statistical averages. The ability to model the anatomy of individuals is essential in understanding the biomechanical underpinnings of conditions affecting the musculoskeletal system because the musculoskeletal system is so highly variable in humans. Being able to visualize the TMJ and analyze the forces exerted on it during normal and abnormal functioning will allow researchers to explore the biomechanical causes of dysfunctional temporomandibular joints in much more detail than they have previously been able to do.

References

- Almodafr, A. 2014. Anatomy and Physiology of the Temporomandibular Joint. Prosthodontics. University of Babylon. www.uobabylon.edu.iq/eprints/publication_9_27180_1641.pdf. Accessed on January 5, 2017.
- Aristeguieta, L.M.R., Acuña, L.E.B. & Ortiz, G.P.S. 2009. A direct anatomical study of the morphology and functionality of disco-malleolar and anterior malleolar ligaments. International Journal of Morphology 27(2): 367-369. <https://pdfs.semanticscholar.org/028b/3a90baad27c97910f9f9c8a35a25de46a990.pdf>. Accessed on April 25, 2017.
- Dutton, M. 2012. Dutton's Orthopedic Examination, Evaluation, and Intervention, 3rd ed. McGraw-Hill Professional Publishing, New York, NY.
- Freemont, A.J. & Hoyland, J. 2006. Lineage plasticity and cell biology of fibrocartilage and hyaline cartilage: Its significance in cartilage repair and replacement. European Journal of Radiology 57(1): 32-36. <https://www-sciencedirect-com.libezp.lib.lsu.edu/science/article/pii/S0720048X05002901?via%3Dihub>. Accessed on April 25, 2018.
- Gray, H. 1918. Anatomy of the Human Body, 20th ed. Lea and Febiger, Philadelphia, PA.
- Gunz, P. 2014. Computed tools for paleoneurology. In: Bruner E. (ed) Human Paleoneurology. Springer Series in Bio-/Neuroinformatics , vol 3. Springer Publishing, Berlin. Pp. 95-120.
- Herring, S. W. 2008. Mechanical Influences on Suture Development and Patency. Frontiers in Oral Biology 12:41-56.

- Herring, S.W., Rafferty, K.L., Liu, Z.J. & Marshall, C.D. 2001. Jaw muscles and the skull in mammals: the biomechanics of mastication. *Comparative Biochemistry and Physiology* 131(1): 207-219.
- Homberger, D.G. 2017. The avian lingual and laryngeal apparatus within the context of the head and jaw apparatus, with comparisons to the mammalian condition: Functional morphology and biomechanics of evaporative cooling, feeding, drinking, and vocalization. Pp. 27-96 in: *The Biology of the Avian Respiratory System: Evolution, Development, Structure and Function* (J. Maina, ed.). Springer-Verlag, New York, NY.
- Homberger, D.G. & Walker, W.F. 2004. *Vertebrate Dissection*, 9th ed. Brooks/Cole, Belmont, CA.
- Lieberman, D.E., McCarthy, R.C., Hiiemae, K.M. & Palmer, J.B. 2001. Ontogeny of postnatal hyoid and larynx descent in humans. *Archives of Oral Biology* 46(2): 117-128.
<https://www.sciencedirect.com/science/article/pii/S0003996900001084>. Accessed on April 26, 2018.
- Ohmure, H., Miyawaki, S., Nagata, J., Ikeda, K., Yamasaki, K. & Al-Kalaly, A. 2008. Influence of forward head posture on condylar position. *Journal of Oral Rehabilitation*. 35:795-800.
- Osborn, M.L. 2013. *The Shoulder Suspension of Bipedal Humans and the Head Suspension of Quadrupedal Cats: A Reconstruction of Macroevolutionary Changes of Complex Systems Based on Natural Experiments, Comparative Anatomy, and Biomechanical Analyses of Extant Organisms*. (Doctoral dissertation) Baton Rouge, LA: Louisiana State University.
https://digitalcommons.lsu.edu/gradschool_dissertations/2485/ Accessed on April 24, 2018.

- Osborn, M.L. & Homberger, D.G. 2015. The evolution of the human shoulder suspension apparatus: Biometrical and biomechanical analyses of right-left asymmetries. *Anatomical Record* 298:1572-1588.
- Osborn, M.L., Rau, A.R.P., Ge, J. & Homberger, D.G. In prep. Free-Body Force Analysis of the Human Shoulder Suspension Apparatus: Development and Comparative Evaluation of 2D and 3D Computational Approaches.
- Patel, T.R. & Collins, J.A. 2016. The Temporomandibular Joint. Pp. 116-123 in: Bergman's Comprehensive Encyclopedia of Human Anatomic Variation, 1st ed. John Wiley & Sons, Inc., Hoboken, NJ.
- Rios, J. & Berman, S. A. 2017. Temporomandibular Disorders. Medscape.
<https://emedicine.medscape.com/article/1143410-overview#showall>. Accessed on October 10, 2017.
- Rocabado, M. & Iglarsh, Z.A. 1991. Musculoskeletal Approach to Maxillofacial Pain. Lippincott Company, Philadelphia, PA.
- Sonnier, B.N. & Homberger, D.G. 2018. 3D Modeling and Animation of the Temporomandibular Joint (TMJ) of a Human Male with Implications for the Study of TMJ Dysfunction. Poster presentation at Experimental Biology April 21-25. Program E137 514.9.
<http://experimentalbiology.org/pdfs-docs/2018/EB-2018-Program.aspx> (page 155)
- Williams, P. 1995. Gray's Anatomy, 38th ed. Churchill Livingstone, London.

Wood, B.M., Jia, G., Carmichael, O., McKlveen, K. & Homberger, D.G. (in press) 3D MRI

Modeling of Thin and Spatially Complex Soft Tissue Structures without Shrinkage:

Lamprey Myosepta as an Example.

Figure Legends

Fig. 1 The isolated temporal bone with its major regions and muscle attachments outlined in red (Gray 1918).

Fig. 2 Sagittal section of the TMJ with the joint capsule, articular disc, and synovial membranes (Gray 1918).

Fig. 3 Lateral 3D view of the mandible with its major components.

Fig. 4 Articular ligaments of the TMJ. Left: Lateral view of the temporomandibular and capsular ligaments. Right: Lateral view of the stylomandibular and sphenomandibular ligaments (Gray 1918).

Fig. 5 The hyoid bone with its major components. A. Frontal view. B. Lateral view. C. Lateral view of the skull, cervical vertebrae, and hyoid bone (in blue).

Fig. 6 Lateral view of the skull showing the location of the temporalis muscle (Gray 1918).

Fig. 7 Lateral view of the neck and facial muscles with the masseter muscle highlighted in dark red (Gray 1918)

Fig. 8 Lateral view of the skull with part of the ramus and the zygomatic arch removed to show the medial and lateral pterygoid muscles (Gray 1918).

Fig. 9 View of the deep muscles of the neck with the digastric muscle highlighted in dark red (Gray 1918).

Fig. 10 Image detailing the difference between high- and low-resolution images in 2D. As seen here, at a lower resolution details smaller than the size of the pixels will not be visible.

(<https://www.mobilebeat.com/getting-familiar-with-images/>)

Fig. 11 Images detailing the process used to replace the old mesh with the newly segmented mesh in Maya 2017®. **A.** View of the segmented bones after the new mesh was exported to Maya 2017®. **B.** Image detailing the process used to “Match Transforms”. Green = material selected first; White = material selected second. **C.** View of the meshes after “Match Transforms” tool was used. **D.** Image detailing the process used to “Replace Objects”. **E.** View after “Replace Objects” tool was used.

Fig. 12 Movements of the lower jaw and corresponding position of the mandibular condyle. **A.** Jaw closed **B.** Jaw half opened. **C.** Jaw fully opened. **D.** Close-up of mandibular condyle at rest in the mandibular fossa. **E.** The mandibular condyle after its anterior angular rotation within the mandibular fossa. **F.** The mandibular condyle after its anterior translation over the articular tubercle of the temporal bone. (Sonnier & Homberger 2018)

Fig. 13 Differential fusion of the anterior portion of the sagittal suture due to post-operative effects. **A.** Superior view of a 3D model of the skull to show the locations of the coronal sections **(B-D)** through the sagittal suture and the successive closure of the suture from cranial to caudal (Sonnier & Homberger 2018)

Figures

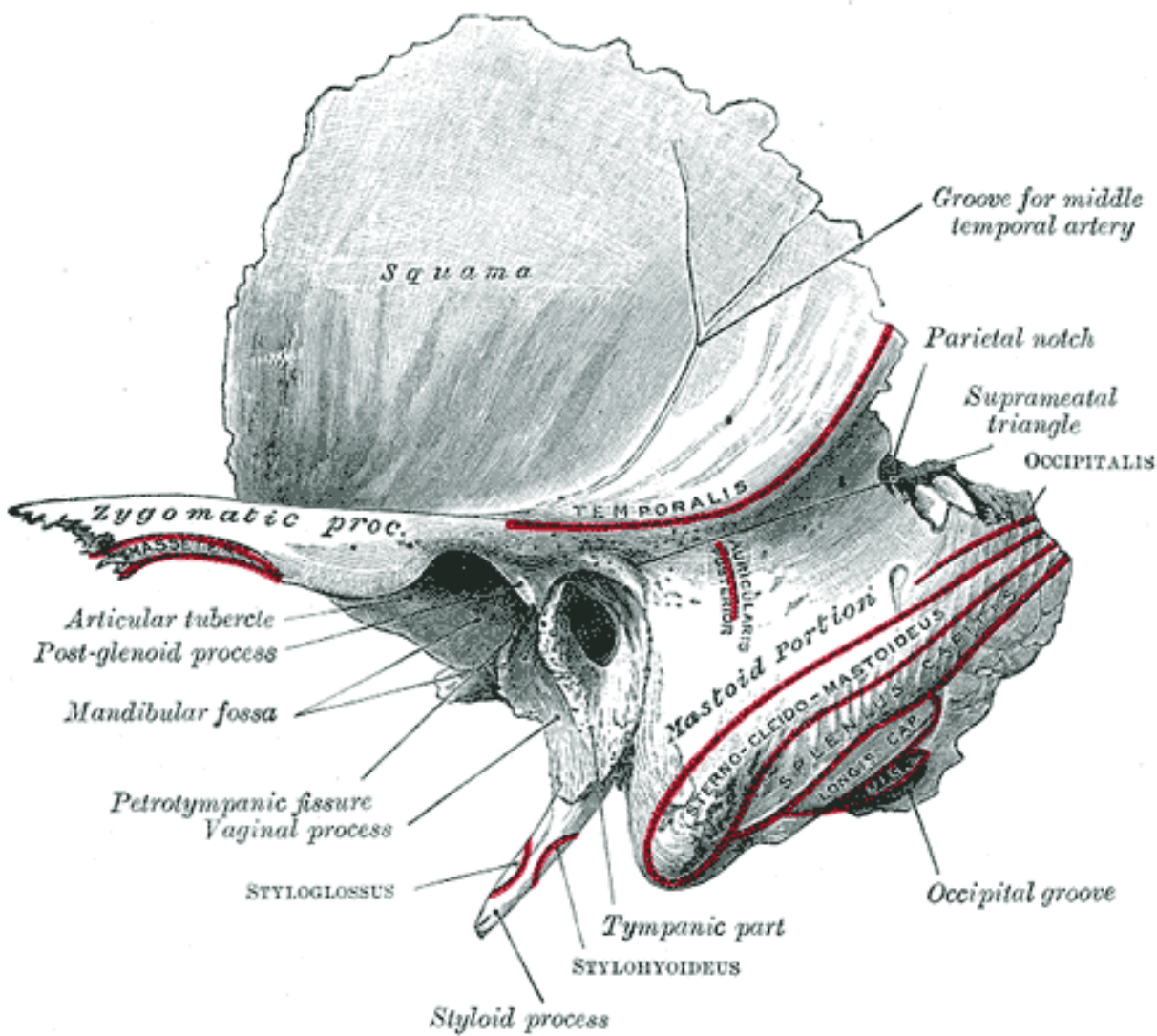


Fig. 1 The isolated temporal bone with its major regions and muscle attachments outlined in red (Gray 1918).

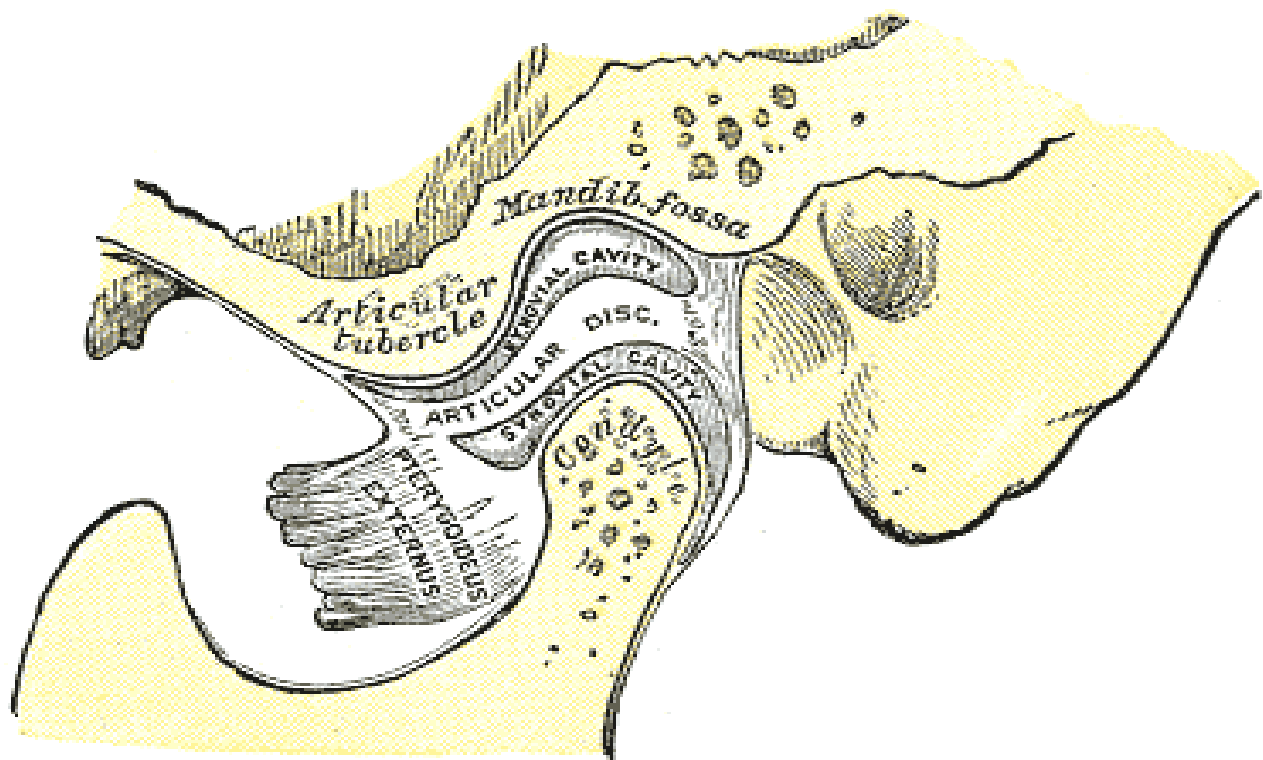


Fig. 2 Sagittal section of the TMJ with the joint capsule, articular disc, and synovial membranes (Gray 1918).

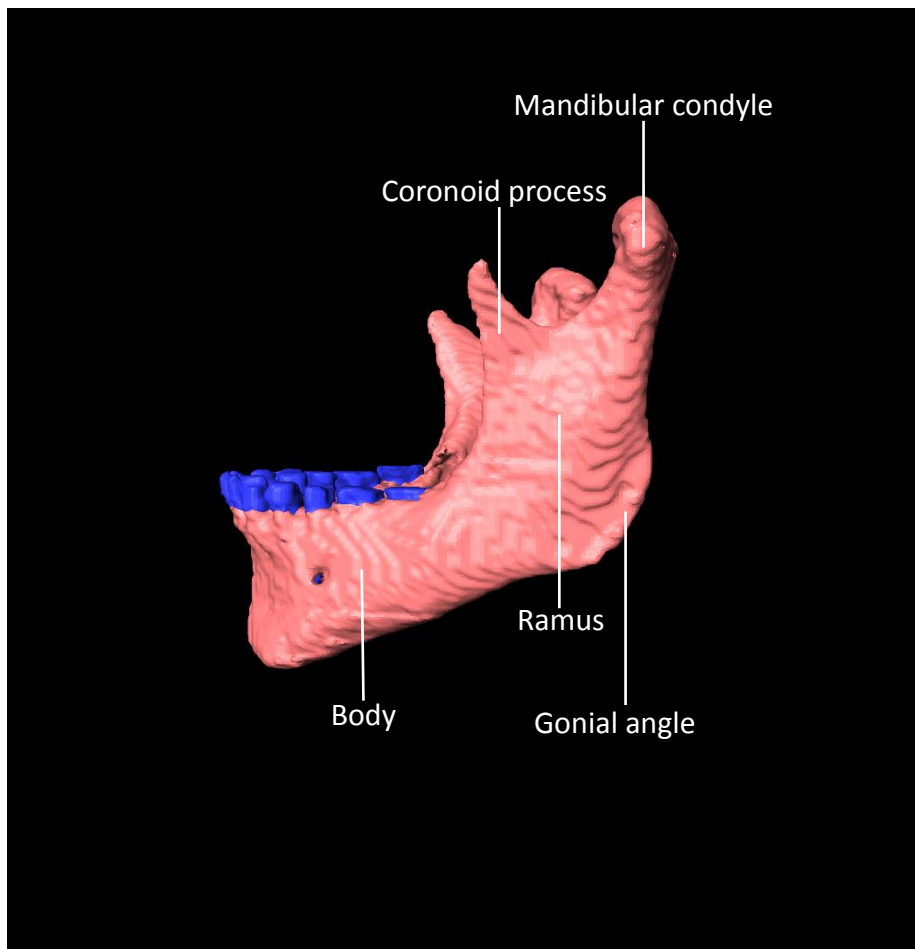


Fig. 3 Lateral view of the mandible with its major components.

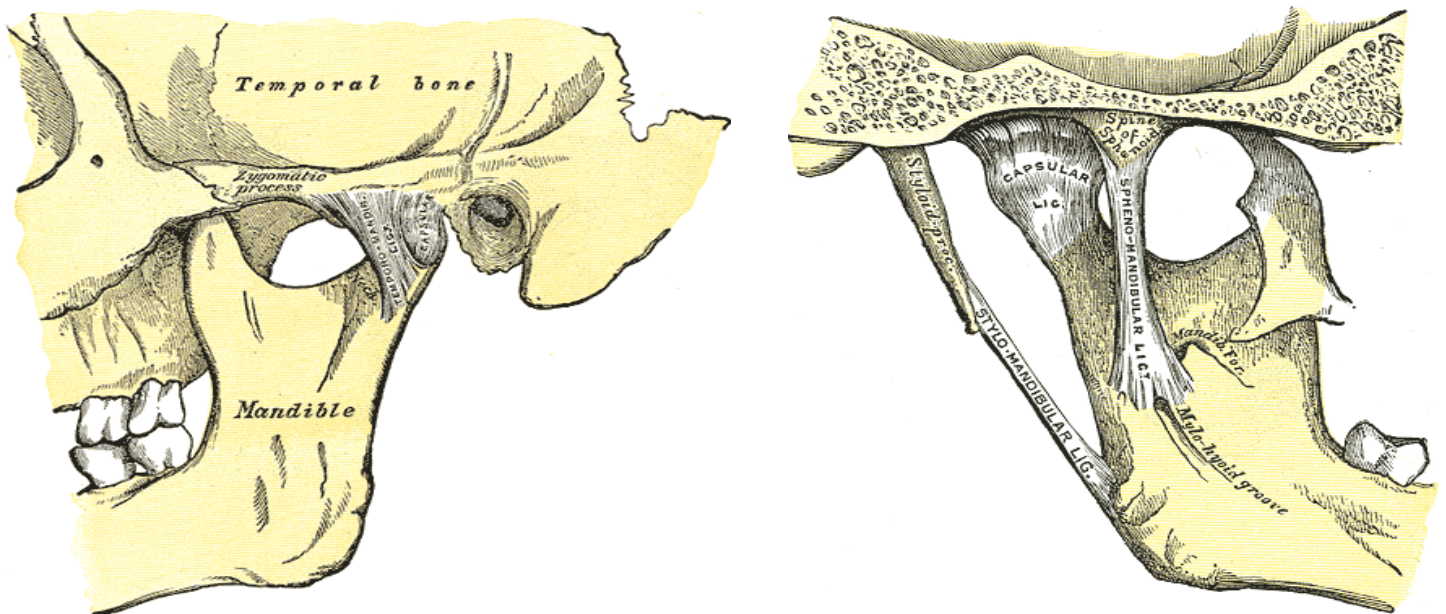


Fig. 4 Articular ligaments of the TMJ. Left: Lateral view of the temporomandibular and capsular ligaments. Right: Lateral view of the stylomandibular and sphenomandibular ligaments (Gray 1918).

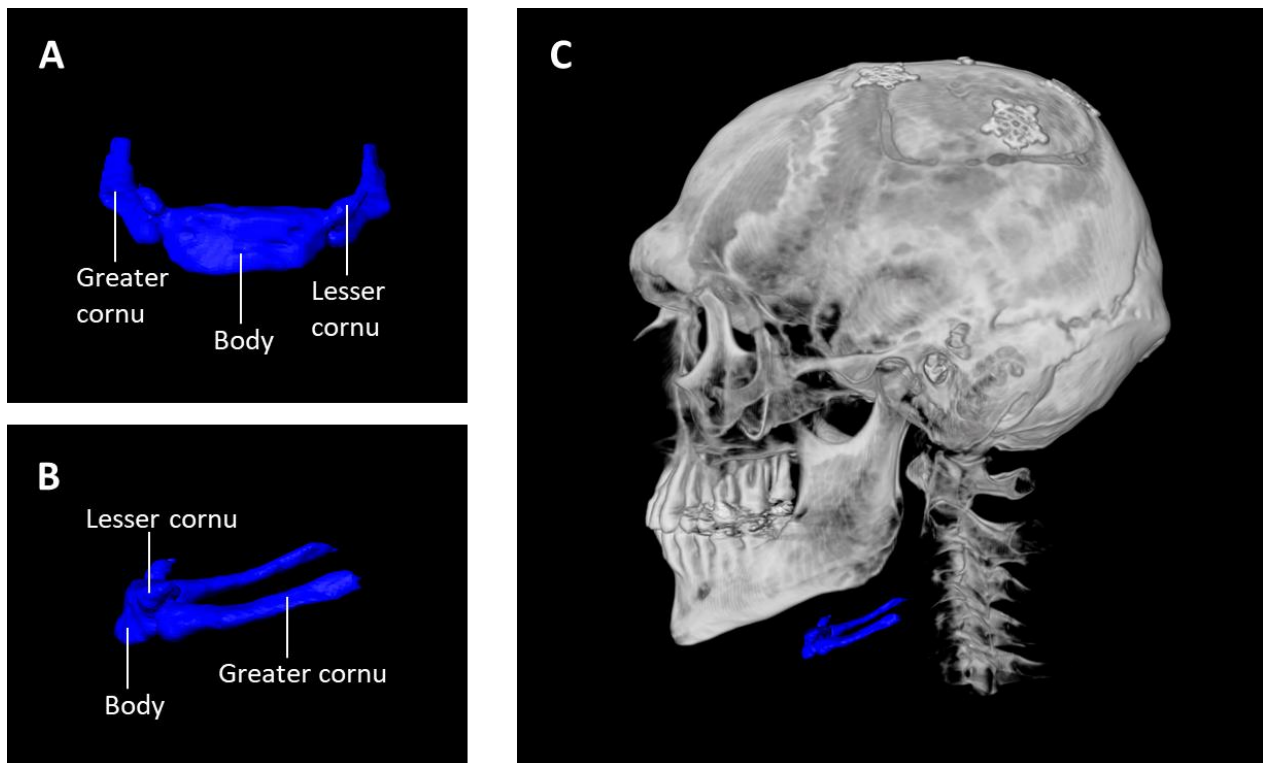


Fig. 5 The hyoid bone with its major components. **A.** Frontal view . **B.** Lateral view. **C.** Lateral view of the skull, cervical vertebrae, and hyoid bone (in blue).

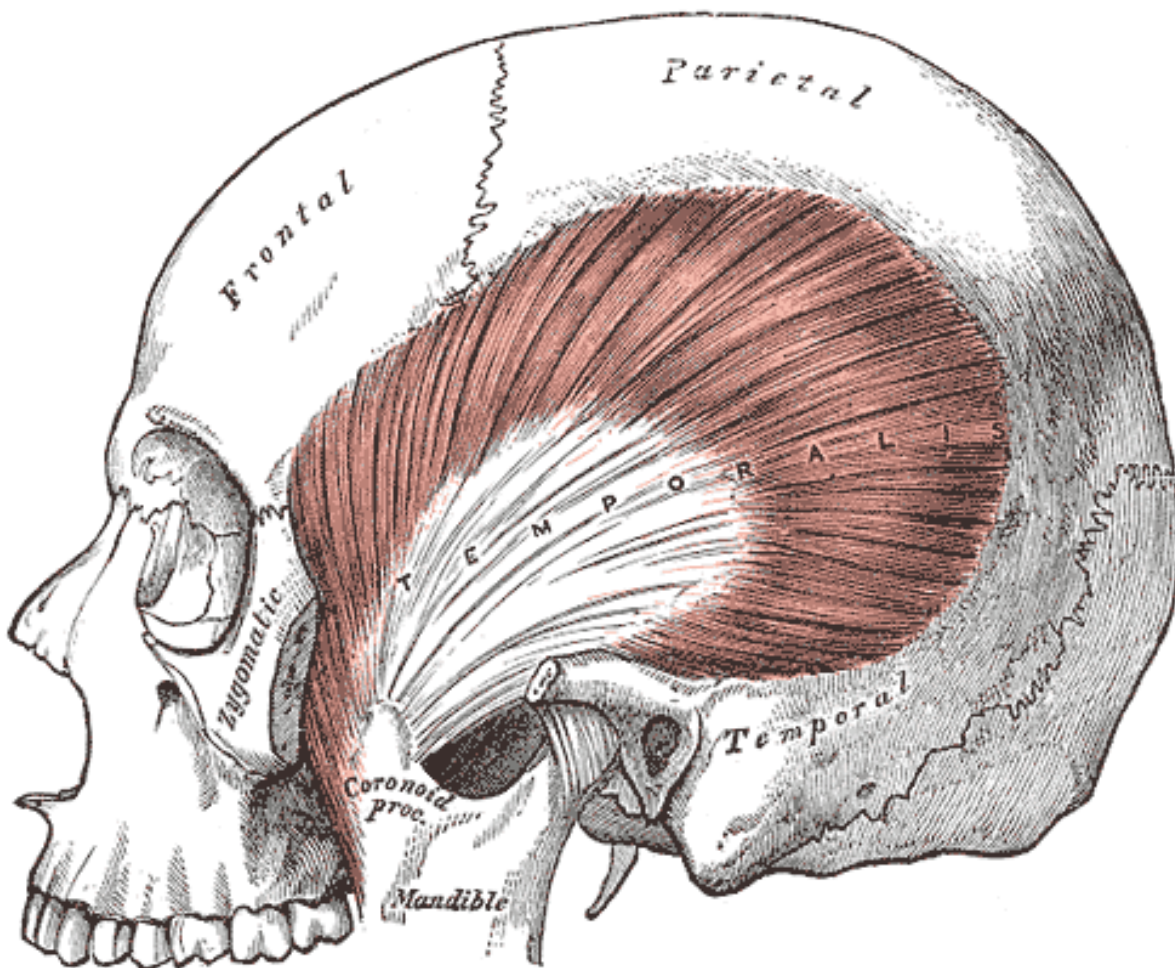


Fig. 6 Lateral view of the skull showing the location of the temporalis muscle (Gray 1918).

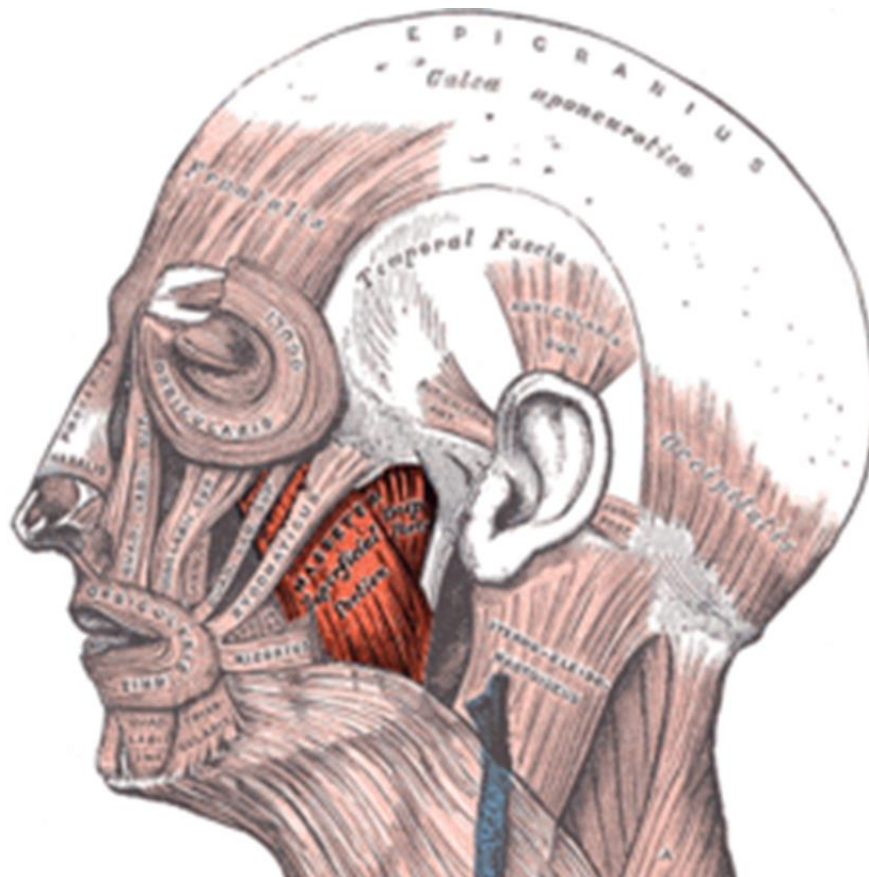


Fig. 7 Lateral view of the neck and facial muscles with the masseter muscle highlighted in dark red (Gray 1918).

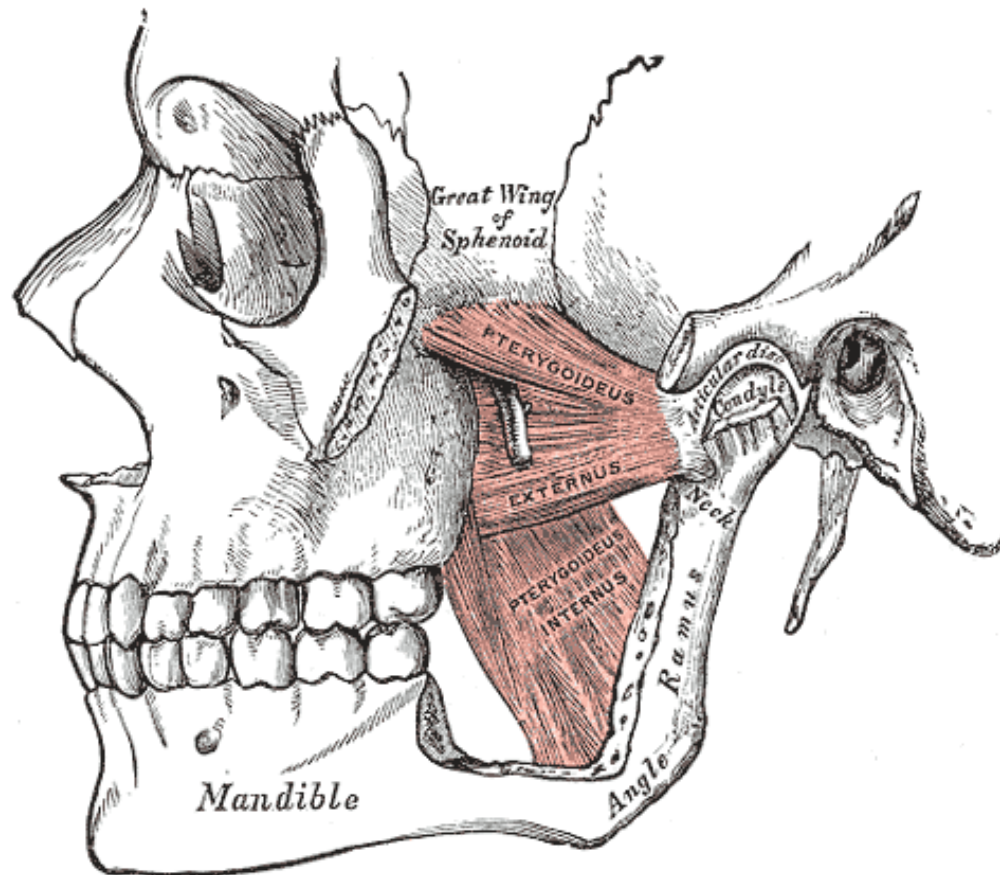


Fig. 8 Lateral view of the skull with parts of the mandibular ramus and zygomatic arch removed to show the medial and lateral pterygoid muscles (Gray 1918).

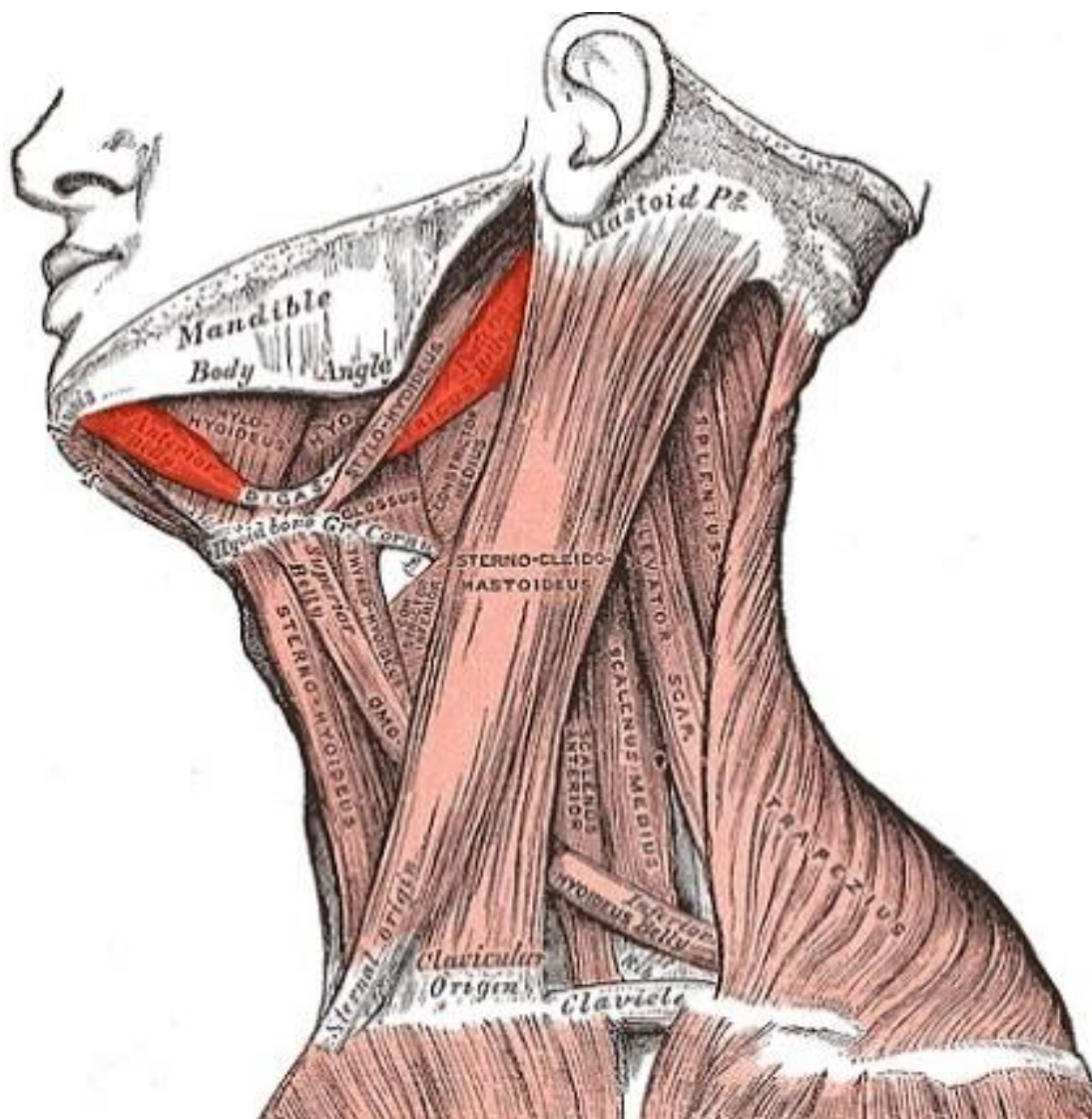


Fig. 9 Lateral view of the deep muscles of the neck with the digastric muscle highlighted in dark red (Gray 1918).

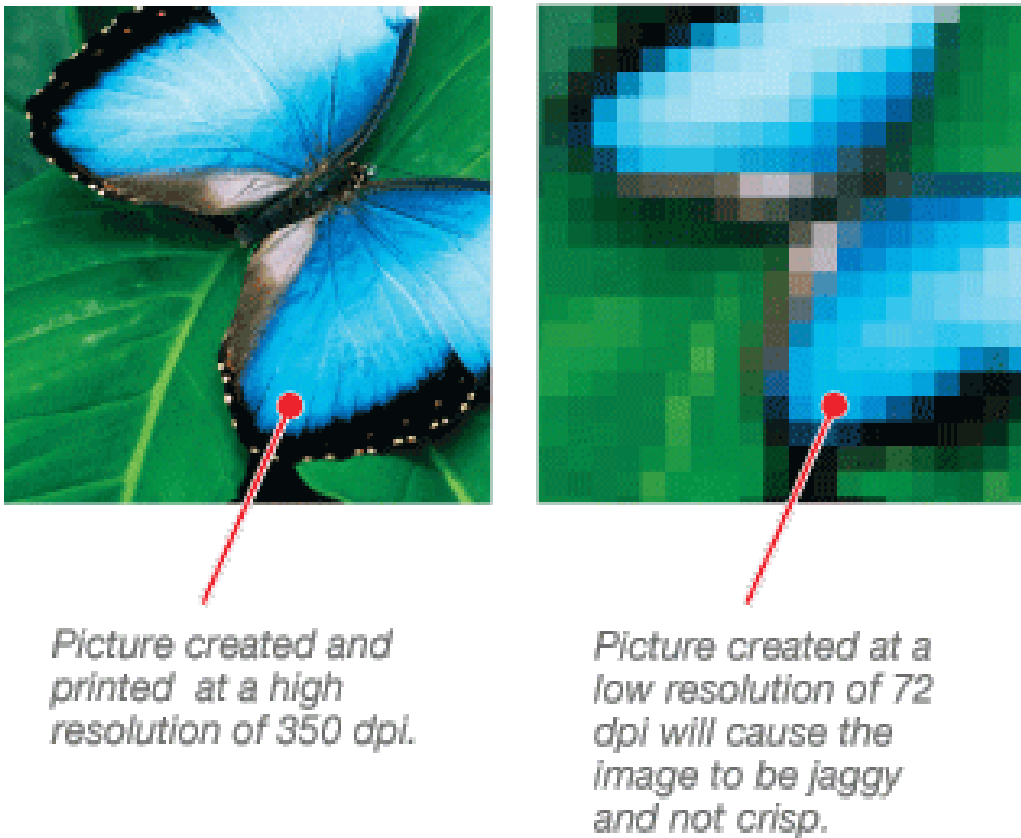


Fig. 10 Image detailing the difference between high- and low-resolution images in 2D. As seen here, at a lower resolution details smaller than the size of the pixels will not be visible. (<https://www.mobilebeat.com/getting-familiar-with-images/>)

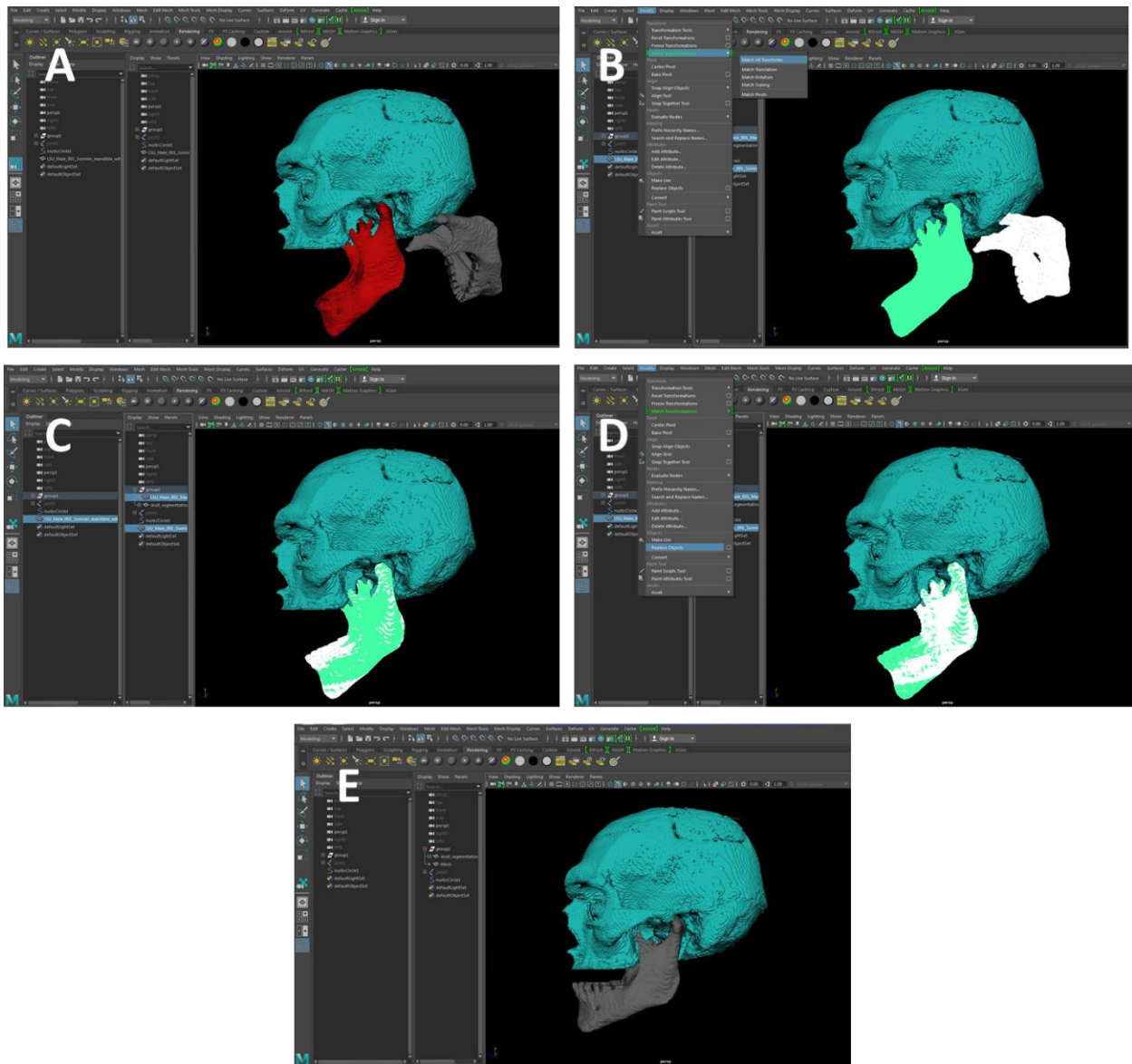


Fig. 11 Images detailing the process used to replace the old mesh with the newly segmented mesh in Maya 2017®. **A.** View of the segmented bones after the new mesh was exported to Maya 2017®. **B.** Image detailing the process used to “Match Transforms”. Green = material selected first; White = material selected second. **C.** View of the meshes after “Match Transforms” tool was used. **D.** Image detailing the process used to “Replace Objects”. **E.** View after “Replace Objects” tool was used.

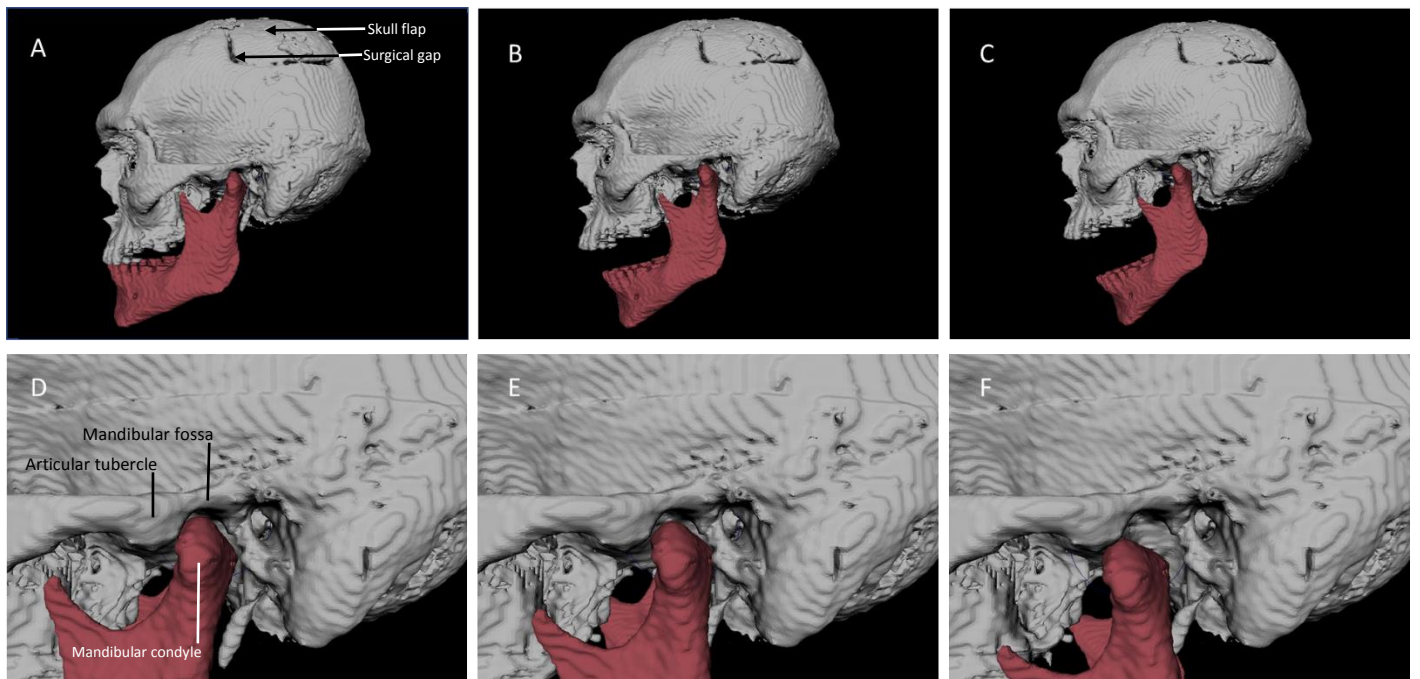


Fig. 12 Movements of the lower jaw and corresponding position of the mandibular condyle. **A.** Jaw closed **B.** Jaw half opened. **C.** Jaw fully opened. **D.** Close-up of mandibular condyle at rest in the mandibular fossa. **E.** The mandibular condyle after its anterior angular rotation within the mandibular fossa. **F.** The mandibular condyle after its anterior translation over the articular tubercle of the temporal bone. (Sonnier & Homberger 2018)

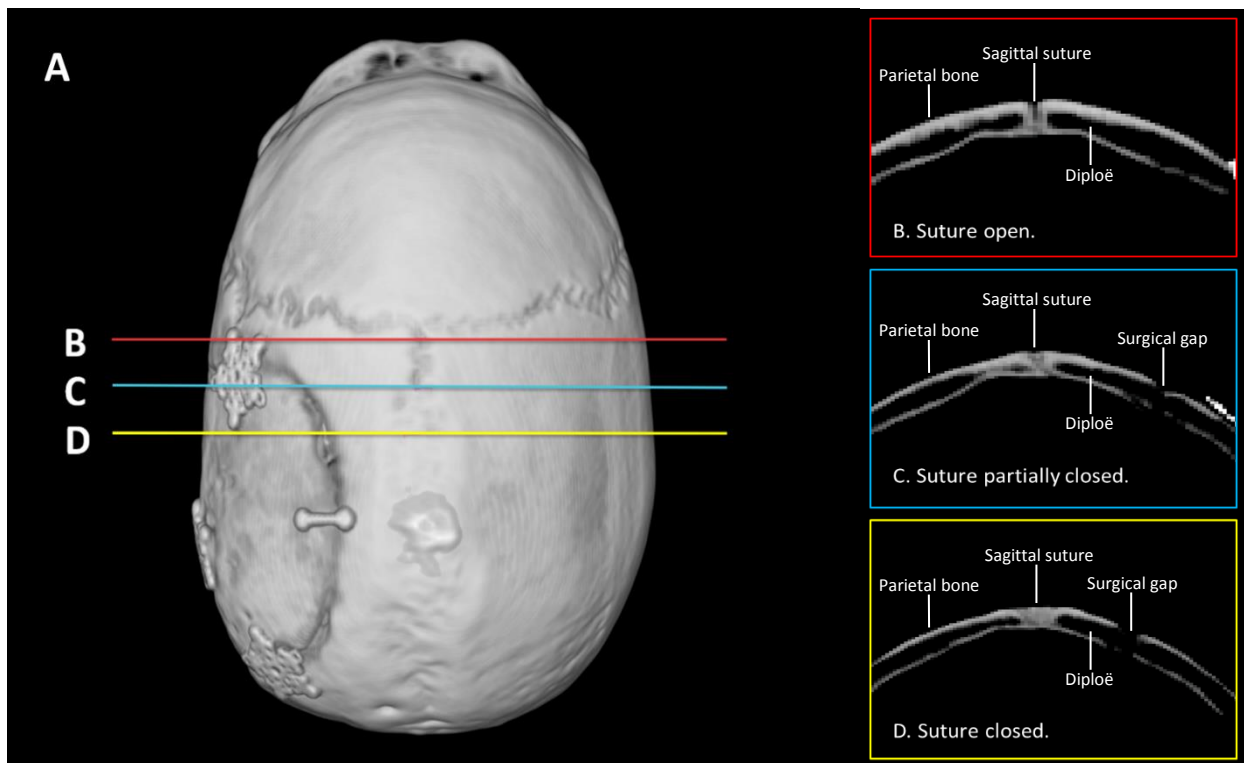


Fig. 13 Differential fusion of the anterior portion of the sagittal suture due to post-operative effects. **A.** Superior view of a 3D model of the skull to show the locations of the coronal sections (**B-D**) through the sagittal suture and the successive closure of the suture from cranial to caudal (Sonnier & Homberger 2018)